DOI: 10.6060/mhc256787s

Novel Imidazolium Derivatives of Thiacalix[4]arenes Containing Fluorescein Fragments: Synthesis, Aggregation Properties and Photocatalytic Activity

Elza D. Sultanova,[@] Alina A. Artemenko, Ekaterina A. Bondareva, Ilshat M. Bogdanov, Aliya E. Akhatova, Diana A. Mironova, Vladimir A. Burilov, Svetlana E. Solovieva, and Igor S. Antipin

Kazan Federal University, 420008 Kazan, Russian Federation
[@]Corresponding author E-mail: elsultanova123@gmail.com

Dedicated to the 90th anniversary of Corresponding Member of Russian Academy Sciences Georgy N. Vorozhtsov

For the first time, p-tert-butyl-thiacalixarene derivatives bearing imidazolium and fluorescein groups on one side and alkyl fragments on the other side of the macrocyclic platform were synthesized. The physicochemical properties of these amphiphilic fluorescein conjugates were thoroughly investigated, revealing the formation of stable aggregates for the octyl-substituted derivative with an average size of approximately 170 nm and a low polydispersity index (0.16). Critical micelle concentrations (CMC) and relative quantum yields were determined using UV-visible absorption and fluorescence spectroscopy. These compounds demonstrated high catalytic activity as photocatalysts in the cross-coupling reaction between N-phenyl-1,2,3,4-tetrahydroisoquinoline and malonic ester in DMF-water solutions. Analysis by gas chromatography–mass spectrometry (GC-MS) and ^{1}H NMR confirmed an exceptional conversion of the starting heterocycle exceeding 96%. The results underscore the potential of these multifunctional thiacalixarenes as highly efficient photocatalysts in aqueous-organic media.

Keywords: Copper-catalysed azide–alkyne cycloadditions (CuAAC), aggregation, macrocyclic fluorescein derivates, photocatalysis.

Новые имидазолиевые производные *п-трет*-бутилтиакаликс[4]арена, содержащие фрагменты флуоресцеина: синтез, агрегационные свойства и фотокаталитическая активность

Э. Д. Султанова,[@] А. А. Артеменко, Е. А. Бондарева, И. М. Богданов, А. Э. Ахатова, Д. А. Миронова, В. А. Бурилов, С. Е. Соловьева, И. С. Антипин

Казанский (Приволжский) федеральный университет, 420008 Казань, Республика Татарстан, Россия
[@]E-mail: elsultanova123@gmail.com

Впервые синтезированы производные п-трет-бутилтиакаликсарена, содержащие имидазолиевые и флуоресцеиновые группы с одной и алкильные фрагменты с другой стороны макроциклической платформы. Физико-химические свойства этих амфифильных конъюгатов с флуоресцеином были тщательно изучены; было установлено, что производное с октильными заместителями образует стабильные агрегаты со средним размером ~170 нм и низким индексом полидисперсности (0.16). Критическая концентрация мицеллообразования (ККМ) и относительные квантовые выходы были определены спектральными методами. Показано, что данные соединения проявляют высокую каталитическую активность в качестве фотокатализаторов в реакции кросс-сочетания между N-фенил-1,2,3,4-тетрагидроизохинолином и малоновым эфиром в растворах ДМФА-вода. Анализ методом газовой хромато-масс-спектрометрии (ГХ-МС) и ^{1}Н ЯМР подтвердил исключительно высокую конверсию исходного гетероцикла, превышающую 96%. Полученные результаты подчер-

кивают потенциал этих многофункциональных тиакаликсаренов в качестве высокоэффективных фотокатализаторов для органических превращений в водно-органических средах.

Ключевые слова: Катализируемые медью азидно-алкиновые циклоприсоединения (CuAAC), агрегация, макроциклические производные флуоресцеина, фотокатализ.

Introduction

As it is well known, developing new methods for creating C–C or C–Het bonds is interesting for modern organic synthesis.[1,2] Classical cross-coupling reactions use both noble metals, which are highly efficient,[3–5] and more affordable nickel.[6–8] The development of new photocatalysts, particularly those that work efficiently in water, is a rapidly developing area in organic chemistry.[9–13] However, the majority of traditional photocatalysts are poorly soluble in aqueous environments,[14,15] that reduces their practical applicability. To address these challenges, researchers are exploring novel materials such as imidazolium calixarenes, which can be fine-tuned to improve their performance in water.[16–19] Incorporating fluorescein groups into these structures not only increases their solubility but also enhances their light-absorbing properties, thereby improving overall photocatalytic efficiency.[20] These new materials hold promise for greener chemical processes, such as water purification, energy conversion, and organic synthesis, without the need for harmful solvents.[21] Furthermore, photo-catalysts that function in water are critical for addressing environmental issues, including the degradation of pollutants[22] and the production of clean hydrogen fuel.[23] Their development is crucial for moving towards sustainable industrial practices. By optimizing the properties of these innovative photocatalysts, we can contribute to the growing need for eco-friendly technologies. Previous studies have also explored the modification of fluorescein to develop chemosensors, biosensors, and catalysts.[20,24]

Previously, derivatives of fluorescein on a thia/calixarene platform bearing various terminal groups were synthesized in our group. Based on these, solid lipid nanoparticles were obtained[25] and/or aggregation[26,27] was studied, and all of these systems were also employed as photocatalysts. In this work, we report the synthesis of a new amphiphilic thiacalixarene platform with fluorescein fragments. These macrocycles incorporate a hydrophilic imidazolium fragment to increase the hydrophilic volume of the amphiphilic molecule. The photophysical properties (quantum yield, fluorescence, and UV absorption), as well as the sizes of the resulting aggregates in a buffer–DMF system, were studied. The photocatalytic activity of the synthesized compounds was investigated in model reactions involving the condensation of N-phenyl-1,2,3,4-tetrahydroisoquinoline with malonic ester.

Experimental

General

Reagents were sourced from Acros or Sigma-Aldrich and used as received without additional purification. Solvents were purified following standard procedures. Synthesis is presented in Scheme 1. The **1a** and **1b**,[28] **2a**, **4a** and 3-azidopropylimidazole (**3**),[29] *o*-propargyl fluorescein (**5**)[30] were synthesized according the literature procedures.

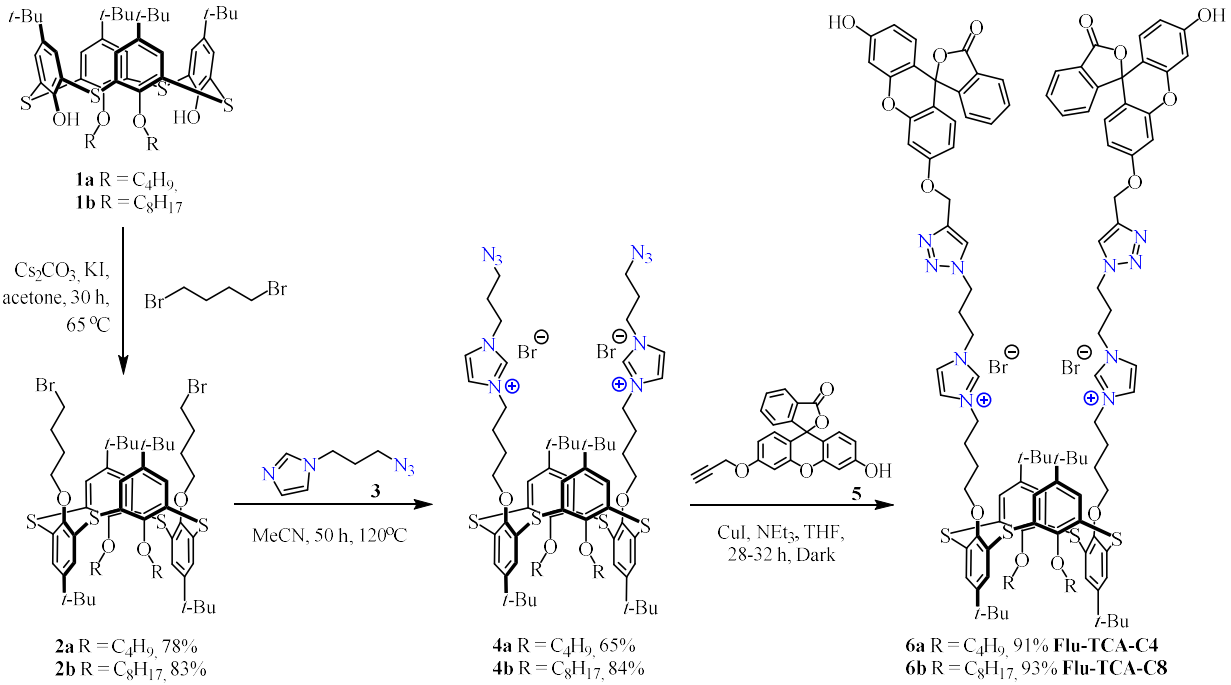

Scheme 1. Synthesis of azide derivatives of 1,2,3-triazole thiacalix[4]arenes (Flu-TCA-C*n*, *n* = 4, 8).

Melting points were measured using the Optimelt MPA100 melting point apparatus (Stanford Research Systems, Sunnyvale, CA, USA). ^{1}H and ^{13}C NMR spectra were recorded on Bruker Avance 400 Nanobay (Bruker Corporation, Billerica, MA, USA) with signals from residual protons of DMSO-d_6 or $CDCl_3$ as internal standard. ATR-IR spectra and IR spectra in KBr pellets were collected using a Infraspek 2202 spectrometer (Infraspek Company, Saint Petersburg, Russia). High-resolution mass spectra with electrospray ionization (HRESI MS) were obtained on an Agilent iFunnel 6550 Q-TOF LC/MS (Agilent Technologies, Santa Clara, CA, USA). Carrier gas: nitrogen, temperature 300 °C, carrier flow rate 12 L·min^{-1}, nebulizer pressure 275 kPa, funnel voltage 3500 V, capillary voltage 500 V, total ion current recording mode, 100–3200 m/z mass range, scanning speed 7 spectra s^{-1}. FTIR spectra were conducted using Bruker Vector-22 using KBr pellets or a thin film in the frequency range of 4000–400 cm^{-1}. TLC was done using Merck UV 254 plates with Vilber Lourmat VL-6.LC UV lamp (6W–254 nm tube). Column chromatography was performed on Merck silica gel (70–230 mesh).

The UV/vis-spectra were recorded on a Shimadzu UV-2600 spectrophotometer (Shimadzu Corporation, Kyoto, Japan) in an optical cell with 10 mm light pass at 298 K.

The mean of micelles size and polydispersity index were determined by dynamic light scattering (DLS) measurement using Malvern ZetaSizer Nano (Malvern Instruments, UK). The source of laser radiation was a He-Ne gas laser with the power of 10 mW and the wavelength of 633 nm. The light scattering angle is 173 °C. The pulse accumulation time is 5–8 min. The signals were analyzed using a single-plate multichannel correlator coupled with IBM PC compatible computer equipped with the software package for the evaluation of effective hydrodynamic radius of dispersed particles. All samples were analyzed in triplicate, the average error of measurements was approximately 4%.

Fluorescence experiments were performed in 10 mm quartz cuvettes and recorded on a Fluorolog FL-221 spectrofluorimeter (HORIBA Jobin Yvon) in the range of 490–625 nm and excitation wavelength 460 nm with 3 nm slit for fluorescein derivatives and in the range of 350–430 nm (excitation wavelength 339 nm with 2.5 nm slit) for pyrene. All measurements were conducted in 1 cm cuvette for fluorescein derivates solutions in water or water-DMF solution. Solutions were prepared using a volume dilution method.

Synthesis

*Compound **2b***. To the solution of the di-substituted **1b** (1.5 g, 1.6 mmol, 1 eq.) in acetone (40 mL) 1,4-dibromobutane (6.912 g, 32 mmol, 20 eq.), following by Cs_2CO_3 (2.06 g, 6.4 mmol, 4 eq.) and KI (0.05 g, 0.32 mmol, 0.2 eq.) were added. The reaction mixture was refluxed for 30 h. After the completion of the reaction the solvent was evaporated in vacuo. The residue was dissolved in dichloromethane, washed with saturated solution of NaCl. The layers were separated and the organic layer was dried over $MgSO_4$, filtered off and evaporated at the reduced pressure. The product was obtained after the dispersion in methanol and the filtering as white solid. Yield 1.58 g, 83%. Mp = 213.5 °C. ^{1}H NMR (400 MHz, $CDCl_3$, 25°C) δ_H ppm: 0.89 (t, J = 8.7 Hz, 6H, CH_3), 0.94 – 1.02 (m, 4H, CH_2CH_3), 1.03– 1.19 (m, 16H, CH_2), 1.20 – 1.25 (m, 8H, $CH_2(CH_2Br)$ + $(OCH_2)CH_2$), 1.27 (s, 18H, $C(CH_3)_3$), 1.29 (s, 18H, $C(CH_3)_3$), 1.61 – 1.71 (m, 4H, $(OCH_2)CH_2$), 3.25 (t, J = 6.8 Hz, 4H, CH_2Br), 3.78 (t, J = 9.4 Hz, 4H, OCH_2), 3.87 (t, J = 7.5 Hz, 4H, OCH_2), 7.30 (s, 4H, HAr), 7.33 (s, 4H, HAr). ^{13}C-{^{1}H} NMR (100.9 MHz, $CDCl_3$, 25°C) δ_C ppm: 14.2, 22.8, 25.0, 28.1, 29.0, 29.38, 29.8, 31.5, 31.6, 31.8, 32.0, 33.5, 34.4, 34.5, 68.2, 68.9, 127.3, 128.0, 128.4, 128.6, 145.7, 145.7157.0, 157.2. IR (KBr) ν_{max} cm^{-1}: 1008 (C–O–C), 1090 (C–Br), ν_s 1260 (C–O–C), 1570 (Ar), 2853 (CH2), 2868 (CH3), 2921 (CH2), 2956 (CH3). HRESI MS (*m/z*) $[M+NH_4]^+$: calcd. for $C_{64}H_{98}Br_2O_4S_4^+$: 1232.4719, found: 1232.4657.

*Compound **4b*** was obtained according the literature procedure,[29] using 1 eq. of **2b** and 2.3 eq. of 1-(3-azidopropyl)-1H-imidazole. Yield: 0.57 g, 84%. Mp = 222.9 °C (with decomp.). ^{1}H NMR (400 MHz, DMSO-d_6, 25 °C) δ_H ppm: 0.85 (br s, 6H, CH_3), 1.11 (br s, 40H, CH_2+$C(CH_3)_3$), 1.77 (br s, 4H, $(OCH_2)CH_2$), 2.07 (br s, 4H, $(OCH_2)CH_2$), 3.44 (br s, 4H, CH_2N_3), 3.74 (br s, 4H, OCH_2), 3.84 (br s, 4H, OCH_2), 4.08 (br s, 4H, CH_2Im), 4.26 (br s, 4H, CH_2Im), 7.31 (s, 4H, ArH), 7.33 (s, 4H, ArH), 7.85 (s, 4H, ImH), 7.89 (s, 4H, ImH), 9.30 (br s, 2H, ImH). ^{13}C-{^{1}H} NMR (101 MHz, DMSO-d_6, 25 °C) δ_C ppm: 13.8, 21.9, 24.9, 25.1, 25.7, 28.6, 28.8, 29.1, 30.8, 31.0, 31.3, 33.8, 33.9, 46.5, 47.6, 47.8, 48.2, 67.8, 68.8, 122.5, 122.6, 127.6, 127.6, 128.0, 128.1, 136.3, 145.2, 145.3, 156.6, 156.8. IR (KBr) ν_{max} cm^{-1}: 1003 (C–O–C), 1263 (C–O–C), 1561 (Ar), 2096 (N_3), 2863 (CH_3), 2926 (CH_2), 2954 (CH_3). HRESI MS (*m/z*) $[M\text{-}2Br^-]^{2+}$: calcd. for $C_{76}H_{112}N_{10}O_4S_4]^{2+}$: 678.3870, found: 678.3870.

*General procedure for synthesis of 1,2,3-triazoles (**6a,b**)*. To a solution of azide **4ab** (1.15 eq.) in 8 mL of THF 0.5 mL of NEt_3 was added following by *o*-propargyl-fluorescein (2 eq.) and CuI (0.1 eq.). The reaction mixture was stirred in the inert atmosphere for 28–32 h. The completion of the reaction was determined by using ^{1}H NMR spectroscopy. After the evaporating the reaction mixture was dissolved in $CHCl_3$ and filtered through Amberlite IRA 67. The resulting solid was dispersed in acetone and then filtered off.

*Flu-TCA-C4 (**6a**)*. Was obtained according to the general procedure from C4-TCA-N_3(a) (0.25 g, 0.17 mmol, 1.15 eq.) and *o*-propargyl-fluorescein (0.115 g, 0.35 mmol, 2 eq.), CuI (0.003 g, 0.015 mmol). Yield: 0.33 g, 91%. Mp = 221 °C (with decomp.). ^{1}H NMR (400 MHz, DMSO-d_6, 25 °C) δ_H ppm: 0.67 – 0.82 (m, 6H, -CH_3), 0.96 – 1.12 (m, 8H, -CH_2-), 1.17 (s, 18H, *t*-Bu), 1.23 (s, 18H, *t*-Bu), 1.72 – 1.81 (m, 4H, -CH_2-), 2.36 – 2.48 (m, 4H, -CH_2-), 3.69 – 3.79 (m, 4H, O-CH_2-), 3.81 – 3.89 (m, 4H, O-CH_2-), 4.06 (t, J = 7.7 Hz, 4H, -CH_2-Im), 4.24 (t, J = 6.9 Hz, 4H, -CH_2-Im), 4.46 (t, J = 6.9 Hz, 4H, -CH_2-Trz), 5.22 (s, 4H, -OCH_2-Flu), 6.48 – 6.72 (m, 4H, ArFlu), 6.72 – 6.89 (m, 4H, ArFlu), 7.11 (d, J = 2.4 Hz, 2H, ArFlu), 7.23 (d, J = 7.4 Hz, 2H, ArFlu), 7.30 (s, 4H, Ar), 7.34 (s, 4H, Ar), 7.69 – 7.77 (m, 4H, ArFlu), 7.81 (d, J = 14.3 Hz, 6H, ImH+ArFlu), 8.00 (d, J = 7.5 Hz, 2H, ArFlu), 8.29 (s, 2H, TrzH), 9.30 (s, 2H, ImH). ^{13}C-{^{1}H} NMR (101 MHz, DMSO-d_6, 25 °C) δ_C ppm: 13.5, 19.1, 22.9, 23.6, 46.4, 50.1, 56.3, 57.9, 60.0, 62.9, 100.5, 104.4, 113.4, 114.2, 116.7, 124.7, 128.8, 129.2, 129.5, 130.0, 130.2, 130.7, 133.3, 133.6, 140.8, 149.6, 153.5, 158.2, 163.8, 164.7, 183.8. IR (KBr) ν_{max} cm^{-1}: 2960, 2870, 1766, 1753 (C=O), 1674 (C-O), 1614, 1477, 1465, 1441, 1353, 1285, 1268, 1246 (C-O-C), 1217, 1182 (C-O-C), 1126, 1108, 1087, 1052, 1028, 1009, 989, 876, 852, 824 (Ar), 796 (Ar). HRESI MS (*m/z*) $[M\text{-}2Br^-]^{2+}$: calcd. for $C_{114}H_{122}N_{10}O_{14}S_4^{2+}$: 991.9024, found: 991.9029.

*Flu-TCA-C8 (**6b**)*. Was obtained according to the general procedure from C8-TCA-N_3(b) (0.3 g, 0.19 mmol, 1.15 eq.) and *o*-propargyl-fluorescein (0.126 g, 0.34 mmol, 2 eq.), CuI (0.003 g, 0.017 mmol). Yield: 0.39 g, 93%. Mp = 124.3 °C (with decomp.). ^{1}H NMR (400 MHz, DMSO-d_6, 25 °C) δ_H ppm: 0.84 (t, J = 7.6 Hz, 6H), 1.18 – 1.20 (m, 56H, -CH_2-+*t*-Bu), 1.38 (s, 4H, -CH_2-), 3.72 – 3.76 (м, 4H, -OCH_2-), 3.87 – 3.88 (m, 4H, -OCH_2-), 4.06 (t, J = 8.0 Hz, 4H, -CH_2-Im), 4.24 (t, J = 7.0 Hz, 4H, -CH_2-Im), 4.46 (t, J = 6.6 Hz, 4H, -CH_2-Trz), 5.22 (s, 4H, -OCH_2-Flu), 6.58 (s, 2H, ArFlu), 6.64 (d, J = 8.9 Hz, 2H, ArFlu), 6.68 – 6.78 (м, 4H, ArFlu), 7.10 (d, J = 2.6 Hz, 2H, ArFlu), 7.30 (s, 4H, Ar), 7.34 (s, 4H, Ar), 7.68 – 7.79 (m, 2H, ArFlu), 7.77 – 7.85 (m, 6H, ArFlu+ImH), 8.00 (d, J = 7.6 Hz, 4H, ArFlu), 8.26 – 8.30 (м, 2H, TrzH), 9.25 (s, 2H, ImH), 10.19 (s, 2H, FluOH). ^{13}C-{^{1}H} NMR (101 MHz, DMSO-d_6, 25 °C) δ_C ppm: 11.1, 14.2, 22.3, 22.7, 23.6, 25.5, 28.7, 29.2, 29.5, 30.1, 31.2, 31.4, 36.5, 38.4, 42.4, 47.0, 53.9, 61.8, 67.8, 101.9, 102.7, 109.7, 111.8, 112.9, 113.4, 120.1, 122.8, 124.4, 125.1, 125.5, 128.9, 129.4, 131.9, 135.6, 136.1, 136.6, 145.7, 152.1, 156.8, 160.2. IR (KBr) ν_{max} cm^{-1}: 3432 (OH), 2948, 2251, 1756 (C=O), 1625 (C-O), 1454, 1380, 1252 (C-O-C), 1183

(C-O-C), 1108, 1056, 1029, 1004, 824 (Ar), 762 (Ar). HRESI MS (*m/z*) $[M\text{-}2Br^-]^{2+}$: calcd. for $C_{122}H_{140}N_{10}O_{14}S_4^{2+}$: 1048.9728, found: 1048.9721.

General procedure of photocatalytic reaction. An optimized procedure was chosen for the photochemical reaction.[31,32] The reagents were mixed in the following concentrations: *N*-phenyl-1,2,3,4-tetrahydroisoquinoline (1 eq., 2.616 mg, 0.0125 mmol), photocatalyst (0.02 eq., 0.00025 mmol), malonic ester (5 eq., 0.01 mL, 0.0625 mmol), and solvent (0.5 mL). The reaction mixture was bubbled with oxygen for 1 minute and allowed to react under blue light illumination (24 w blue-LED photoreactor) for 5–16 hours. The solvent was evaporated under reduced pressure (8 mm Hg, 90 °C).

Results and Discussion

Synthesis of 1,2,3-triazoles derivatives of thiacalix[4]arenes (Flu-TCA-Cn, n = 4, 8)

The initial compounds for the synthesis of target molecules were *di*-substituted **1ab** thiacalixarenes with lipophilic side chains, which were obtained through the Mitsunobu reaction.[28] In the next step, *tetra*-substituted macrocycles **2a,b** in the stereoisomeric form of *1,3-alternate* were obtained with good yields by reacting with a 15-fold excess of 1,4-dibromobutane in the presence of Cs_2CO_3 (Figure S1). Subsequently, macrocycles **2a,b** were reacted with 2.3 equivalents of azidopropylimidazole **3** in acetonitrile at 120 °C. The reaction mixture was stirred for 36 hours and the target compounds **4a,b** were isolated with yields of 65% and 84%, respectively. The structures of the newly synthesized compounds were confirmed and characterized using various physical techniques. In the infrared (IR) spectra of imidazolium macrocyclic compounds, a strong absorption band was observed around 2100 cm^{-1} (Figure S2c), attributed to the asymmetric stretching vibrations of the azide functional group. High-resolution mass spectrometry (HRESI-MS) data obtained using electrospray ionization revealed peaks corresponding to quasi-molecular ions of macrocycle **4b** (Figure S2d), with cleavage of two bromine atoms (for **4b**: found 678.3870, calcd. for $[C_{76}H_{112}N_{10}O_4S_4]^{2+}$: 678.3870).

The Cu(I)-catalyzed azide-alkyne cycloaddition (CuAAC) reaction[33] was employed to introduce fluorescein moieties into the synthesized macrocyclic structures. Fluorescein acetylene, the *o*-propargyl ether of fluorescein molecule **5**, served as the starting material for the reaction.

The reaction was carried out in THF at room temperature using catalytic quantities of copper iodide (CuI) and triethylamine (NEt_3) as a base. ^{1}H NMR spectroscopy was used to monitor the progress of the reaction, which took approximately 48 hours to complete. The reaction mixture was concentrated under vacuum, dissolved in chloroform, and filtered through an ion-exchange resin (Ambrlite IRA 67) to remove any residual copper ions. After evaporation and dispersion in acetone, the desired compounds **6a** and **6b** (TCA-Flu-C4 and TCA-Flu-C8, respectively) were obtained with yields of 91–93%.

In the HRESI spectra of compounds **6a,b** signals corresponding to doubly charged quasi-molecular ions resulting from the cleavage of halogen atoms were observed. For the macrocycle **6a**: found *m/z* 991.9029, calcd. for $C_{114}H_{122}N_{10}O_{14}S_4^{2+}$ 991.9024 (Figure S3d); for the macrocycle **6b**: found *m/z* 1048.9721, calcd. for $C_{122}H_{140}N_{10}O_{14}S_4^{2+}$ 1048.9728 (Figure S4c).

The ^{1}H NMR spectra revealed the presence of new signals, such as a triazole proton signal at δ = 8.28 ppm, as well as a shift in the signal for methylene protons of the linker between fluorescein and the triazole fragments, from 5.20 to 5.22 ppm. Additionally, other signals associated with the fluorescein moiety could be observed in the aromatic region of the NMR spectrum (Figure S4a).

Spectral and aggregation properties of compounds Flu-TCA-Cn, n = 4, 8)

The presence of a xanthene dye fragment determines the fluorescent properties of the resulting compounds. Compounds **5**, Flu-TCA-C4 and Flu-TCA-C4 are well soluble in DMF. The fluorescence spectra of these molecules in DMF were studied upon increasing the Tris buffer (10 mM) content, where the percentage of buffer varied from 0% to 100%. DMF solutions do not exhibit significant fluorescence (Figure 1A). The addition of buffer resulted in an increase in the fluorescence intensity of both Flu-TCA-C4 and Flu-TCA-C8, with a maximum at a 50% buffer fraction. This fluorescence enhancement suggests the formation of aggregates at this specific DMF-buffer ratio.

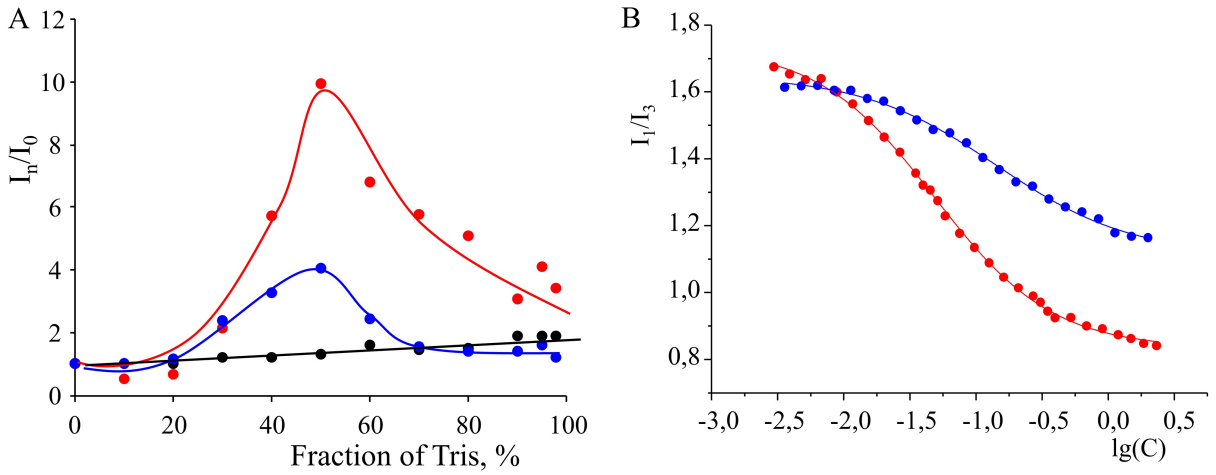

Figure 1. Dependence of the emission intensity (A) on the Tris content (C = 0.2 mM) and (B) Plot of I_1/I_3 pyrene emission *vs* the concentration of **5** (black), Flu-TCA-C4 (blue) and Flu-TCA-C8 (red).

Table 1. CMC values, average hydrodynamic diameters and PDI for **5**, Flu-TCA-C4 and Flu-TCA-C8 in DMF 50%.

Compound	CMC, mM	Concentration, mM	PDI	Z-average, nm
5	-	0.008–0.5	-	-
Flu-TCA-C4	0.14	0.008	0.274±0.02	910±36
		0.08	0.474±0.034	943±12
		0.2	-	-
		0.5	-	-
Flu-TCA-C8	0.05	0.008	0.400±0.008	212±0.6
		0.08	0.167±0.012	164±1
		0.2	0.170±0.001	165±2
		0.5	0.163±0.009	215±0.3

To test the hypothesis that aggregation occurs at this DMF-buffer ratio, the critical micelle concentrations of the fluorescein derivatives were determined. This was accomplished by monitoring the change in the pyrene I_1/I_3 fluorescence intensity ratio – a sensitive measure of local polarity – as a function of concentration (50% DMF). The resulting sigmoidal curves (Figure 1B), fitted to a Boltzmann model (Table S1), yielded the CMC values listed in Table 1. A clear trend was observed: the CMC decreases with increasing length of the lipophilic chain, consistent with enhanced hydrophobicity (Table 1). The correlation between fluorescence intensity and the concentration of the obtained fluorescein derivates was also studied. It is worth noting that, as the concentration increases, a significant increase in fluorescence intensity was observed (Figure S5). This indicates that this structure do not lead to self-quenching with increasing concentration, which makes it possible to obtain an aggregation-induced emission system.[34-36]

Aggregation of compounds was studied by dynamic light scattering (DLS) method (Table 2). Increasing the concentration of Flu-TCA-C8 results in a decrease of Polydispersity Index (PDI) and aggregate size, whereas Flu-TCA-C4 forms large size associates with high PDI values in the concentration range 0.008–0.08 mM. In the case of **5**, as expected, no associates were detected. Flu-TCA-C8 forms associates with a smaller hydrodynamic diameter and PDI due to the hydrophobic effects of long alkyl fragments.

Table 2. Relative fluorescence quantum yield of fluorescein derivatives in Tris-DMF and DMF.

	5	Flu-TCA-C4	Flu-TCA-C8
Q_s, (50% DMF)	69	47	65
Q_s, (DMF)	60	17	10

One of the most important characteristics in evaluating the photophysical properties of fluorescent molecules is quantum yield (Qs), which is calculated as the ratio of photons emitted to the number of photons absorbed.[37,38] Using the relative calculation method, according to Equation (1), the quantum yield of compound **5** and fluorescein derivatives, relative to the disodium salt of fluorescein, was calculated:

$$Q_S = Q_r\left(\frac{m_S}{m_r}\right)\left(\frac{n_S}{n_r}\right)^2 \quad (1),$$

where Q_s is the fluorescence quantum yield of an unknown sample, Q_r is the quantum fluorescence yield of a known standard, m_s and m_r are the gradients of the integrated fluorescence intensity plot versus absorption (Figure S6), n_s and n_r are the refractive indices of the solvents used for the unknown and reference samples, respectively. Whereas the absolute quantum yield of the disodium salt fluorescein is 95% (0.1 M NaOH),[39] the relative quantum yields of fluorescein compounds were calculated from measurements of fluorescence and absorption in DMF and aqueous DMF solutions (50 % DMF) (Table 2).

When switching to solutions with a lower DMF content, the quantum yield of fluorescence emission shows a slight decrease. This is due to the ability of fluorescein derivatives to form H- and J-aggregates, which affects their optical properties.[40] According to the Kascha theory,[41] the type of dye aggregates can be identified by the shift of the absorption maximum in the spectrum of the dimer relative to that of the monomer: H-type aggregates (face-to-face type) exhibit a hypsochromic (blue) shift of the absorption maximum, whereas the formation of J-aggregates results in a bathochromic shift. Figure 2 shows the absorption and emission spectra for the studied compounds at different concentrations (monomer and dimer), normalized to the same height for clarity. As shown in the emission spectra (Figure 2b), increasing the concentration of fluorescein leads to a hypsochromic shift, while its derivatives display a bathochromic shift, indicating the formation of J-aggregates. In the absorption spectra, this effect is not observed when increasing the concentration from 0.008 mM to 0.2 mM; however, when comparing the fluorescein derivatives based on thiacalixarene with compound **5**, a bathochromic shift is evident and more pronounced for Flu-TCA-C8. Additionally, in the absorption spectra of fluorescein derivatives the absorption maximum shifts bathochro-

mically relative to fluorescein (Figure 2a), indicating the change in the polarity of the microenvironment and is consistent with the solvatochromic behavior of fluorescein,[18] indirectly pointing to the formation of aggregates.

To determine the conversion of the initial THI during the reaction, gas chromatography–mass spectrometry (GC-MS) and ^{1}H NMR were used. This involved constructing the calibration curve of the peak area of THI versus its concentration to calculate the conversion (Figure S9). In the ^{1}H NMR spectra, the conversion was assessed by comparing the relative intensities of two protons from the CH_2-group in the α-position of the starting THI (appearing as a singlet at 4.27 ppm) and one proton from a CH-group between the CO_2ET groups in the target product, appearing as a doublet at 5.57 ppm (Figure S10). A difference of 1-8% was observed between the ^{1}H NMR and GC-MS results when comparing the data. According to the data obtained, the use of a calixarene platform results in a more efficient reaction and provides near 100% conversion within 5 hours of blue light irradiation (Table 3).

The difference in activity can be attributed to the macrocyclic effect, which is associated with the preorganization and spatial separation of fluorescein molecules. This prevents deactivation of the excited species and facilitates electron transfer.[44–46] Additionally, the calix[4]arenes platform acts as a nanoreactor,[47,48] concentrating reagents within the cavity between fluorescein molecules, that results in a more effective action of the photocatalytic components of the molecule.[49–51] This is supported by the consistent catalytic activity observed in macrocyclic systems regardless of their specific structure when tested in aqueous–DMF solutions. In pure DMF, the catalytic activity of the systems decreases, which is consistent with the data on relative quantum yield. Fluorescein and compound **5** have the highest quantum yield, but macrocyclic derivatives showed the best efficiency in the reaction, that indicates a micellar effect in the DMF-water reaction.

Table 3. The conversion and yield based on GC-MS and ^{1}H NMR data for the reaction of the addition of malonic ester to the α-position of THI, 5 h.

Photocatalyst	Solvent	Conversion, % (GC-MS)	Yield, % (^{1}H NMR)
Fluorescein	DMF:water (1:1)	84	88
	DMF	80	78
5	DMF:water (1:1)	94	80
	DMF	68	62
Flu-TCA-C4	DMF:water (1:1)	94	96
	DMF	53	57
Flu-TCA-C8	DMF:water (1:1)	95	99
	DMF	61	72
No catalyst	DMF	0	0

Photocatalytic activity of fluorescein derivatives

Photocatalysis has become a versatile tool for C-H activation reactions of sp^3-hybridized carbon atoms, enabling direct and selective C-C bond formation.[42] As a model reaction to evaluate the catalytic activity of compound **5**, Flu-TCA-C4 and Flu-TCA-C8, the cross-coupling of N-phenyl-1,2,3,4-tetrahydroisoquinoline (THI) with malonic ester[43] in the presence of blue light was studied (Scheme 2). A custom-built photoreactor equipped with blue light-emitting diodes (LEDs) at a wavelength of 460 nm and a total output power of 24 W, with air cooling to ensure efficient operation was employed (Figure S8).

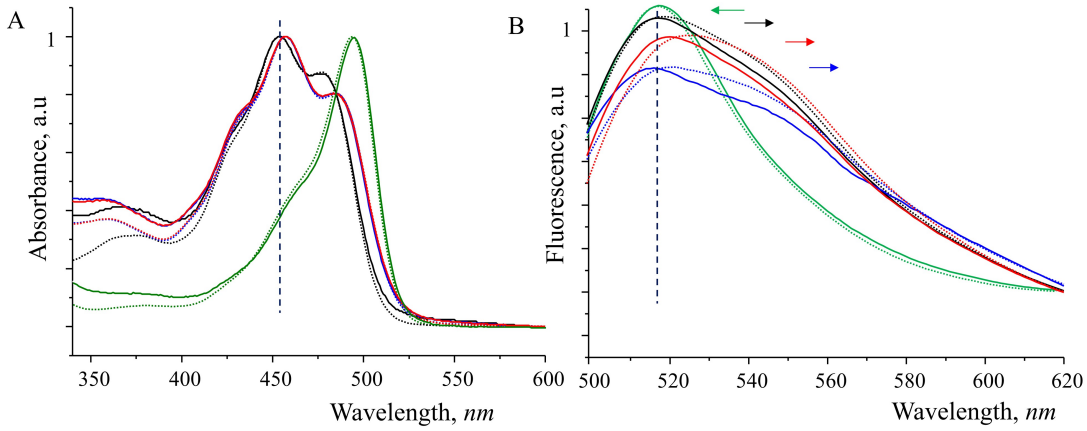

Figure 2. Absorption and (B) emission spectra of fluorescein (green), **5** (black), Flu-TCA-C4 (blue), Flu-TCA-C8 (red) in water:DMF=1:1, *C*=0.2 mM (dot); *C*=0.008 mM (solid).

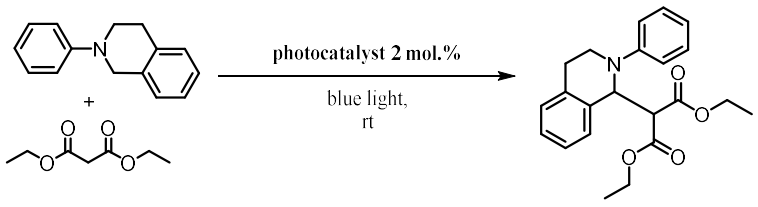

Scheme 2. Photocatalytic addition of malonic ester to THI.

Conclusions

Novel photocatalysts based on *p*-*tert*-butylthiacalix[4]arene derivatives containing imidazolium and fluorescein fragments were synthesized. These new materials exhibited high catalytic activity in a model reaction involving THI and malonic ester, achieving a 99% yield of the desired product when performed in a water–DMF mixture. The efficiency of new catalysts surpasses that of initial fluorescein and *o*-propargyl–fluorescein due to the presence of a macrocyclic structure and the ability of the calixarene scaffold to concentrate reactants. The incorporation of imidazole groups and fluorescent labels into the catalysts structure holds promise for future applications in molecular recognition and as highly effective photocatalyst in water. The introduction of the imidazolium group into the fluorescein-containing thiacalixarene led to the formation of stable associates in the case of compounds with octyl fragments. Based on these findings, AIE materials with potential for various applications, primarily in biomedicine and materials science, may be developed.

Acknowledgements. This work was supported by a grant from the Academy of Sciences of the Republic of Tatarstan, awarded to young Candidates of Sciences (postdoctoral researchers) to facilitate the defense of their doctoral dissertations, conduct research, and fulfill professional duties in scientific and educational institutions within the Republic of Tatarstan. The grant was provided under the State Program of the Republic of Tatarstan, 'Scientific and Technological Development of the Republic of Tatarstan.'

Author Contribution. Elza D. Sultanova: Writing – original draft; Writing – review and editing; Funding acquisition. Alina A. Artemenko: Visualization; Investigation; Writing - Original Draft. Ekaterina A. Bondareva: Investigation. Ilshat M. Bogdanov: Investigation; formal analysis. Aliya E. Akhatova: Investigation; formal analysis. Diana A. Mironova: Investigation; Conceptualization. Vladimir A. Burilov: Project administration. Svetlana E. Solovieva: Supervision. Igor S. Antipin: Supervision

References

1. Raghavan P., Rago A.J., Verma P., Hassan M.M., Goshu G.M., Dombrowski A.W., Pandey A., Coley C.W., Wang Y. *J. Am. Chem. Soc.* **2024**, *146*, 15070–15084, doi: 10.1021/jacs.4c00098.
2. Datta S., Chandra A., Bhattacharya S. *Inorg. Chim. Acta* **2024**, *572*, 122249, doi: 10.1016/j.ica.2024.122249.
3. Srivastava A., Kaur H., Pahuja H., Rangarajan T.M., Varma R.S., Pasricha S. *Coord. Chem. Rev.* **2024**, *507*, 215763, doi: 10.1016/j.ccr.2024.215763.
4. Horbaczewskyj C.S., Fairlamb I.J.S. *Org. Process Res. Dev.* **2022**, *26*, 2240–2269, doi: 10.1021/acs.oprd.2c00051.
5. Firsan S.J., Sivakumar V., Colacot T.J. *Chem. Rev.*, **2022**, *122*, 16983–17027, doi: 10.1021/acs.chemrev.2c00204.
6. Bagherzadeh N., Reza Sardarian A. *J. Photochem. Photobiol. A Chem.*, **2024**, *449*, 115345, doi: 10.1016/j.jphotochem.2023.115345.
7. Gesmundo N.J., Rago A.J., Young J.M., Keess S., Wang Y. *J. Org. Chem.*, **2024**, *89*, 16070–16092, doi: 10.1021/acs.joc.3c02351.
8. Su L., Gao S., Chen L., Yan J., Jiang Y., Zheng Q., Liu J. *Chem. – An Asian J.*, **2025**, *20*, doi: 10.1002/asia.202500214.
9. Zhdanova K.A., Vyal'ba F.Y., Bragina N.A. *Macroheterocycles* **2024**, *17*, 150–179, doi: 10.6060/mhc245875z.
10. Oleinikova V.A., Khomyakov T.D., Polivanovskaia D.A., Birin K.P., Tsivadze A.Y. *Macroheterocycles* **2025**, *18*, 92–98, doi: 10.6060/mhc256653b.
11. Lee D.-E., Kim M.-K., Danish M., Jo W.-K. *Catal. Commun.* **2023**, *183*, 106764, doi: 10.1016/j.catcom.2023.106764.
12. Saeed M., Muneer M., ul Haq A., Akram N. *Environ. Sci. Pollut. Res.* **2022**, *29*, 293–311, doi: 10.1007/s11356-021-16389-7.
13. Liu S., Wang M., He Y., Cheng Q., Qian T., Yan C. *Coord. Chem. Rev.* **2023**, *475*, 214882, doi: 10.1016/j.ccr.2022.214882.
14. Ray A.K., Beenackers A.A.C. *Catal. Today* **1998**, *40*, 73–83, doi: 10.1016/S0920-5861(97)00123-5.
15. Lee S.-H., Kang M., Cho S.M., Han G.Y., Kim B.-W., Yoon K.J., Chung C.-H. *J. Photochem. Photobiol. A Chem.* **2001**, *146*, 121–128, doi: 10.1016/S1010-6030(01)00553-6.
16. Sultanova E.D., Gafiatullin B.K., Ocherednyuk E.A., Garipova R.I., Volodina A.A., Daminova A.G., Evtugyn V.G., Burilov V.A., Solovieva S.E., Antipin I.S. *Macroheterocycles* **2023**, *16*, 168–176, doi: 10.6060/mhc235118s.
17. Ling I., Campbell C.L., Sobolev A.N., Dalgarno S.J. *CrystEngComm* **2022**, *24*, 4201–4207, doi: 10.1039/D2CE00459C.
18. Ocherednyuk E.A., Garipova R.I., Bogdanov I.M., Gafiatullin B.K., Sultanova E.D., Mironova D.A., Daminova A.G., Evtugyn V.G., Burilov V.A., Solovieva S.E., Antipin I.S. *Colloids Surfaces A Physicochem. Eng. Asp.* **2022**, *648*, 129236, doi: 10.1016/j.colsurfa.2022.129236.
19. Burilov V., Garipova R., Mironova D., Sultanova E., Bogdanov I., Ocherednyuk E., Evtugyn V., Osin Y., Rizvanov I., Solovieva S., Antipin I. *RSC Adv.* **2021**, *11*, 584–591, doi: 10.1039/D0RA 09740C.
20. Tu X.-P., Wei L.-L., Zhang K.-X., Chen Y., Zhou M.-D. *Tetrahedron* **2024**, *160*, 134028, doi: 10.1016/j.tet.2024.134028.
21. Armaković S.J., Savanović M.M., Armaković S. *Catalysts* **2022**, *13*, 26, doi: 10.3390/catal13010026.
22. a) Abhishek B., Jayarama A., Rao A.S., Nagarkar S.S., Dutta A., Duttagupta S.P., Prabhu S.S., Pinto R. *Int. J. Hydrogen Energy* **2024**, *81*, 1442–1466, doi: 10.1016/j.ijhydene.2024.07.262; b) Medvedeva I.V., Medvedeva O.M., Studenok A.G., Studenok G.A., Tseytlin E.M. *ChemChemTech* [*Izv. Vyssh. Uchebn. Zaved. Khim. Khim. Tekhnol.*] **2023**, *66*(1), 6–27, doi: 10.6060/ivkkt.20236601.6538.
23. Ahmad K., Ghatak H.R., Ahuja S.M. *Environ. Technol. Innov.* **2020**, *19*, 100893, doi: 10.1016/j.eti.2020.100893.
24. Rajasekar M. *J. Mol. Struct.* **2021**, *1224*, 129085, doi: 10.1016/ j.molstruc.2020.129085.
25. Burilov V.A., Artemenko A.A., Garipova R.I., Amirova R.R., Fatykhova A.M., Borisova J.A., Mironova D.A., Sultanova E.D., Evtugyn V.G., Solovieva S.E., Antipin I.S. *Molecules* **2022**, *27*, 2436, doi: 10.3390/molecules27082436.
26. Burilov V., Fatykhova A., Mironova D., Sultanova E., Nugmanov R., Artemenko A., Volodina A., Daminova A., Evtugyn V., Solovieva S., Antipin I. *Molecules* **2022**, *28*, 261, doi: 10.3390/molecules28010261.
27. Artemenko A., Sultanova E., Mironova D., Akhatova A., Bondareva E., Islamov D., Usachev K., Solovieva S., Burilov V., Antipin I. *Organics* **2024**, *5*, 346–360, doi: 10.3390/org5030018.

28. Burilov V., Nugmanov R., Ibragimova R., Solovieva S., Antipin I. *Mendeleev Commun.* **2015**, *25*, 177–179, doi: 10.1016/j.mencom.2015.05.005.
29. Burilov V., Garipova R., Sultanova E., Mironova D., Evtugyn V., Osin Y., Solovieva S., Antipin I. *Macroheterocycles* **2019**, *12*, 340–345, doi: 10.6060/mhc191174b.
30. Chen Tai-Shan, Zhu Jing, Wu Houming, Yao Zhu-Jun L.H. *Synlett* **2006**, *2006*, 1225–1229, doi: 10.1055/s-2006-941564.
31. Hari D.P., König B. *Org. Lett.* **2011**, *13*, 3852–3855, doi: 10.1021/ol201376v.
32. Franz J.F., Kraus W.B., Zeitler K. *Chem. Commun.* **2015**, *51*, 8280–8283, doi: 10.1039/C4CC10270C.
33. Makarov E., Iskhakova Z., Burilov V., Solovieva S., Antipin I. *J. Incl. Phenom. Macrocycl. Chem.* **2023**, *103*, 355–368, doi: 10.1007/s10847-023-01202-4.
34. Feng S., Gong S., Feng G. *Chem. Commun.* **2020**, *56*, 2511–2513, doi: 10.1039/C9CC09784H.
35. Singh V.K., Prasad R., Koch B., Hasan S.H., Dubey M. *New J. Chem.* **2017**, *41*, 5114–5120, doi: 10.1039/C7NJ00106A.
36. Sharma V.S., Patel U., Thakar S., Rathod S.L., Sharma A.S., Shrivastav P.S., Athar M. *New J. Chem.* **2023**, 47, 1444–1459, doi: 10.1039/D2NJ05133H.
37. Collins K.D., Washabaugh M.W. *Q. Rev. Biophys.* **1985**, *18*, 323–422, doi: 10.1017/S0033583500005369.
38. *Principles of Fluorescent Spectroscopy* (Lakowicz J., Ed.) **2006**, Springer New York, NY, 954 p., doi: 10.1007/978-0-387-46312-4.
39. Shen J., Snook R.D. *Chem. Phys. Lett.* **1989**, *155*, 583–586, doi: 10.1016/0009-2614(89)87477-9.
40. Das S., Chattopadhyay A.P., De S. *J. Photochem. Photobiol. A Chem.* **2008**, *197*, 402–414, doi: 10.1016/j.jphotochem.2008.02.003.
41. Kasha M. *Radiat. Res.* **1963**, *20*, 55, doi: 10.2307/3571331.
42. Beil S.B., Bonnet S., Casadevall C., Detz R.J., Eisenreich F., Glover S.D., Kerzig C., Næsborg L., Pullen S., Storch G., Wei N., Zeymer C. *JACS Au* **2024**, *4*, 2746–2766, doi: 10.1021/ jacsau.4c00527.
43. Liu Q., Li Y., Zhang H., Chen B., Tung C., Wu L. *Chem. – A Eur. J.* **2012**, *18*, 620–627, doi: 10.1002/chem.201102299.
44. Kim J.S., Quang D.T. *Chem. Rev.* **2007**, *107*, 3780–3799, doi: 10.1021/cr068046j.
45. Zhao B.-T., Zhu X.-M., Chen X.-H., Yan Z.-N., Zhu W.-M. *Chinese Chem. Lett.* **2013**, *24*, 573–577, doi: 10.1016/j.cclet.2013.04.026.
46. Harriman A., Hissler M., Jost P., Wipff G., Ziessel R. *J. Am. Chem. Soc.* **1999**, *121*, 14–27, doi: 10.1021/ja982786v.
47. Syah R., Zahar M., Kianfar E. *Int. J. Chem. React. Eng.* **2021**, *19*, 981–1007, doi: 10.1515/ijcre-2021-0069.
48. Mironova D., Bogdanov I., Akhatova A., Sultanova E., Garipova R., Khannanov A., Burilov V., Solovieva S., Antipin I. *Int. J. Mol. Sci.* **2023**, *24*, 16663. doi: 10.3390/ijms242316663.
49. Parisi C., Ferreri L., Martins T.J., Laneri F., Sollima S., Azzolina A., Cusimano A., D'Antona N., Consoli G.M.L., Sortino S. *Beilstein Arch.* **2025**, 202513, doi: 10.3762/bxiv.2025.13.v1.
50. Di Bari I., Granata G., Consoli G.M.L., Sortino S. *New J. Chem.* **2018**, *42*, 18096–18101, doi: 10.1039/C8NJ03704C.
51. Sarkar P., Mukhopadhyay C. *Green Chem.* **2016**, *18*, 442–451, doi: 10.1039/C5GC01859E.

Received 08.10.2025
Accepted 21.10.2025